

## Carbon nanotube Y junctions: growth and properties

L.P. Biró<sup>a,\*</sup>, Z.E. Horváth<sup>a</sup>, G.I. Márk<sup>a</sup>, Z. Osváth<sup>a</sup>, A.A. Koós<sup>a</sup>, A.M. Benito<sup>b</sup>, W. Maser<sup>b</sup>,  
Ph. Lambin<sup>c</sup>

<sup>a</sup>Research Institute for Technical Physics and Materials Sciences, P.O. Box 49, H-1525 Budapest, Hungary

<sup>b</sup>Instituto de Carboquímica (CSIC), C/Miguel Luesma Castán 4, E-50015 Saragossa, Spain

<sup>c</sup>Laboratoire de Physique du Solide, Facultes Universitaires Notre-Dame de la Paix, B-5000 Namur, Rue de Bruxelles 61, Belgium

### Abstract

An overview of the available data on carbon nanotube Y junctions is given. The structural models and the transport calculations on the Y junctions are reviewed followed by the various methods, which successfully produced these junctions and the available experimental transport and tunneling data of the grown junctions. In the discussion section, the common and different features of the various growth methods are analyzed and some particularities of branched nano-objects are outlined, which have to be taken account in the interpretation of the tunneling data.

© 2003 Elsevier B.V. All rights reserved.

**Keywords:** Carbon nanotubes; Y junctions; Growth; Structure; Electronic transport; Tunneling

### 1. Introduction

The increasing number of papers on novel, complex carbon nanotube type nanoarchitectures like multiwall [1] and singlewall Y junctions [2], simple [3] and multiple coiled nanotubes [4,5] clearly shows that the  $sp^2$  hybridization of carbon makes possible a large variety of tubular, carbon based nanostructures. These new structures are potential building blocks of an ‘all-carbon’ nanoelectronics. Such a circuitry, in which the interconnects to the macroscopic world are significantly reduced in number, will fully exploit the nanometer size of its components. To be able to achieve this, networks of interconnected carbon nanotubes have to be constructed. For constructing a network the simplest basic building elements one can use are Y or T junctions either achieved during nanotube growth [6–8], or by later processing steps like functionalization and interconnections through chemical bonds [9,10].

The purpose of the present paper is to overview the available data on the growth and properties of the carbon nanotube Y junctions produced during nanotube growth, the junctions produced by chemical interlinking are not

within the scope of the present paper. The paper is organized as follows: first the structural models and the transport calculations on the Y junctions are reviewed followed by the various methods, which successfully produced these junctions and the available experimental transport and tunneling data of the grown junctions. In Section 4 the common and different features of the various growth methods are analyzed and some particularities of branched nano-objects are outlined, which have to be taken account in the interpretation of the tunneling data.

### 2. Structural models and calculated transport properties

#### 2.1. Structure

The first structural models for symmetric carbon nanotube Y junctions based on theoretical calculations [11,12] were proposed shortly after the discovery of multiwall carbon nanotubes by Iijima [13]. Both models are based on the insertion of non-hexagonal (n-H) rings (at least six heptagons) in the hexagonal network in the region where the three branches of the Y are joined together. All the subsequent structural models [14–19] follow the same construction principle of conserving the  $sp^2$  hybridization of the carbon network, differing only

\*Corresponding author. Tel.: +36-1-3922681; fax: +36-1-3922226; <http://www.mfa.kfki.hu/int/nano>.

E-mail address: [biro@mfa.kfki.hu](mailto:biro@mfa.kfki.hu) (L.P. Biró).

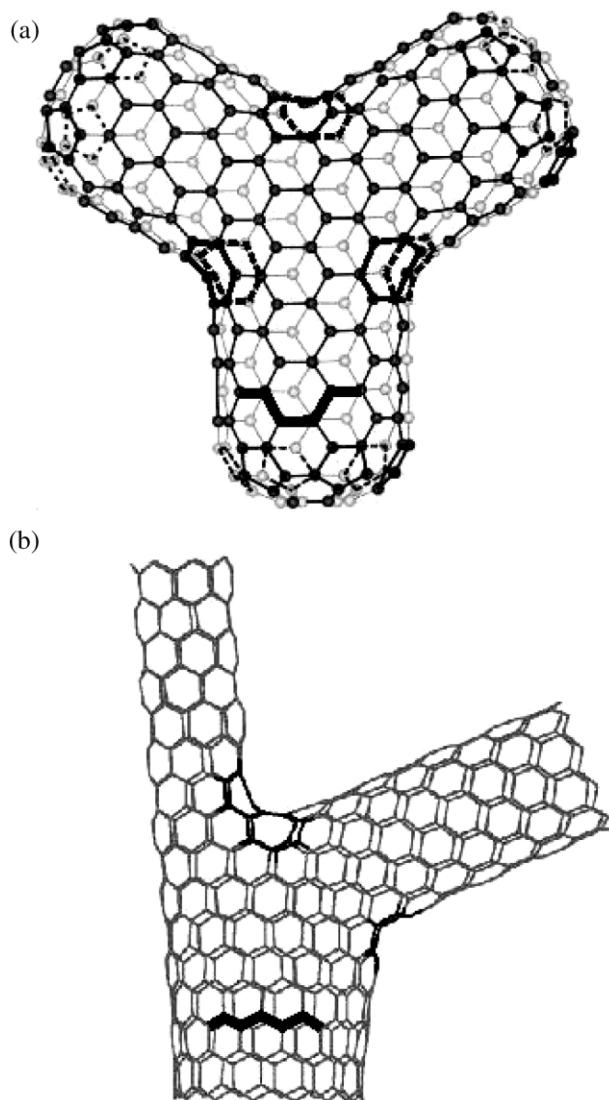


Fig. 1. Structural models of carbon nanotube Y junctions. (a) Symmetric, armchair Y junction as proposed by Scuseria [11], the six heptagons are highlighted in black; (b) asymmetric, zig-zag Y junction after [18], n-H rings highlighted in black.

in the kind, number and placement of the n-H rings. These variations make possible the constructions of various symmetric and asymmetric model junctions [18] and various angles from Y to T shapes [14]. A Y junction is named symmetric if the three carbon nanotubes joining each other in the Y have identical chirality and the distribution of the n-H rings around the Y is symmetric. Such a junction will be constituted from identical branches oriented at  $120^\circ$ , like in Fig. 1a. Whenever one of the above conditions is not fulfilled the junction will be asymmetric, a possible example is shown in Fig. 1b. The case of asymmetric junctions is somewhat more complex as in this case various combinations of metallic and semiconductor tubes can be built. Even an asymmetric Y built only of semiconductor

carbon nanotubes, but with different diameters, may exhibit rectification effects due to the different gap values associated with the different diameters leading to the formation of a system similar to semiconductor heterojunctions in the Y [20].

## 2.2. Conductance

Nonconducting bias windows may appear in the Y junction region, even for symmetric junctions built of metallic carbon nanotubes due to the number of the n-H rings and due to the way in which they are arranged [15]. Treboux and co-workers have calculated the properties of a series of spacer elements in the junction regions, which they call ‘triangulenes’, Fig. 2. According to their model the complete Y junction is treated as being composed of three semiinfinite, metallic (12, 0) zig-zag carbon nanotubes joined by the triangulene units and the necessary n-H rings to conserve the  $sp^2$  connectivity of the carbon lattice. According to their calculations if the triangulene spacer has an atom centered on the  $C_3$  symmetry axis, Fig. 2a, it exhibits no conduction

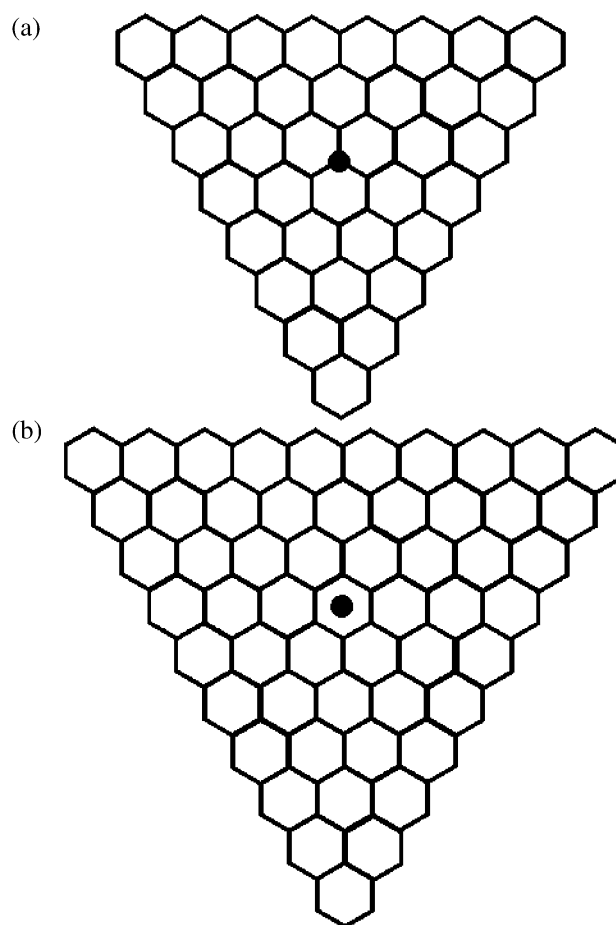


Fig. 2. Triangulene spacers as proposed in [15] to join three metallic zig-zag carbon nanotubes into an Y junction. (a) Triangulene with atom centered  $C_3$  axis; (b) ring centered  $C_3$  axis.

gap, only an electron hole asymmetry, but when the triangulene spacer has a ring centered on the  $C_3$  axis, Fig. 2b, a characteristic gap is found in the conductance [15]. Every third increase of the size of triangulene spacer (every increase is done by increasing the number of the hexagons along the edge of the spacer by one) results in a spacer with ring centered  $C_3$  axis. The existence of the conduction gap is associated with LDOS differences arising in the two kinds of spacers, the central region of the triangulene spacer with ring centered  $C_3$  axis loses the metallic character.

### 2.3. Rectification

The rectification in the Y junction is a somewhat controversial issue. Andriotis et al. [18] calculated the quantum conductivity for a large number of Y junctions using the Landauer formalism [21] based on a Green's function method. Not only the nanotube branches of the Y junctions are taken into account, but also the effect of the metallic leads. The effect arising due to the metallic leads are introduced by calculating the self energy term for those carbon atoms which are situated on the interface plane between the nanotube and its Ni (001) lead [18]. Two main groups of structures are studied: (a) junctions with no change of chirality and (b) change of chirality on branching. The authors conclude that in accordance with Treboux's findings the rectification and switching depend strongly on the symmetry of the spacer connecting the three branches and, to a lesser degree, on chirality [18]. They find: (i) perfect rectification is obtained for symmetric carbon nanotube junctions consisting of zig-zag stems; (ii) asymmetric Y junctions show no rectification; (iii) Y junctions containing armchair stems, although having asymmetric  $I$ - $V$  characteristics, exhibit small leakage currents for positive bias; (iv) perfect rectification and switching properties are intrinsic properties of the Y junctions exhibiting specific symmetry and consisting of zig-zag stems. Using a similar calculation method, in a recent work, Meunier et al. [19] bring arguments that the rectification in a symmetric junction is not an intrinsic property of the branching, but it is solely due to the properties of the interface between the nanotube branches and the metallic leads. The rectification is attributed to Schottky-type interface states and the magnitude of the effect is found to be strongly dependent on the detailed atomic geometry of the contact [19]. In addition, it seems now well established that the electronic properties of a nanotube/lead interface depend strongly on contamination, especially with oxygen [22].

From the point of view of carbon nanotube based nanoelectronic circuitry, both kinds of Y junctions are needed: ones that show no rectification for interconnects and ones that show rectification for being used as active elements.

## 3. Experimental results

### 3.1. Growth of Y junctions

#### 3.1.1. Electric arc

The first observation of carbon nanotube Y junctions was reported in an electric arc experiment. The junctions found by transmission electron microscopy (TEM) were short branched, multiwall ones [23]. The arc discharge was operated under He atmosphere at 660 mbar and a current density of 220 A/cm<sup>2</sup> was used at a 27 V DC bias. A hollow, cylindrical graphite rod of 0.64 cm with a hole of 0.32-cm diameter was used as anode, no filling was present in the hollow core of the anode. The deposit from the cathode was collected and analyzed by TEM, junctions of various shapes L, T and Y were found. The HRTEM images show that in the branches the graphitic layers are oriented parallel with the tube axis, while in the junction region they have 'saddle-like' shape.

Recently in a DC electric arc experiment carried out in 660 mbar He, also using a hollow anode, of 6-mm diameter, drilled out to have a cylindrical, axial hollow of 3.5 mm in diameter and filled with a nickel/yttrium mixture (resulting in an overall graphite/nickel/yttrium composition of 90/7/3 wt.% over the drilled-out length) single and few wall Y junctions were found by scanning tunneling microscopy (STM) in the cathodic deposit together with straight multiwall carbon nanotubes and nanotube knees with diameters typically approximately 10 nm [24]. The Y junctions found are asymmetric, usually have a stem of larger diameter, the ratio of the diameter of the stem to the diameter of the branches is in the range of 1.5–4, the apparent diameters of the stems as measured from the height of the tubes over the substrate are in the range of 0.3–1 nm. Taking into account that the measured values of the apparent heights in STM measurements are affected by several distorting factors [25–27], which cause the reduction of the real diameter, these values strongly suggest single or few wall branches. The observed Y junctions usually show growth instabilities and sometimes kinks, too, before branching, a typical example of such a Y junction is shown in Fig. 3, some of the growth instabilities are marked by white arrows.

STM and scanning tunneling spectroscopy (STS) measurements were reported recently on nanotube samples prepared by the electric arc method. Neither the exact location from which the sample was collected within the reaction chamber, nor the arc discharge parameters were given in detail [28]. An asymmetric Y junction was measured in topographic mode and by STS. The apparent heights of the three branches are: 0.45, 0.4 and 0.35 nm, respectively. The same observation is valid concerning the real diameters as in the previous paragraph [25–27]. The diameter values obtained from the STS data indicate tubes with surpris-

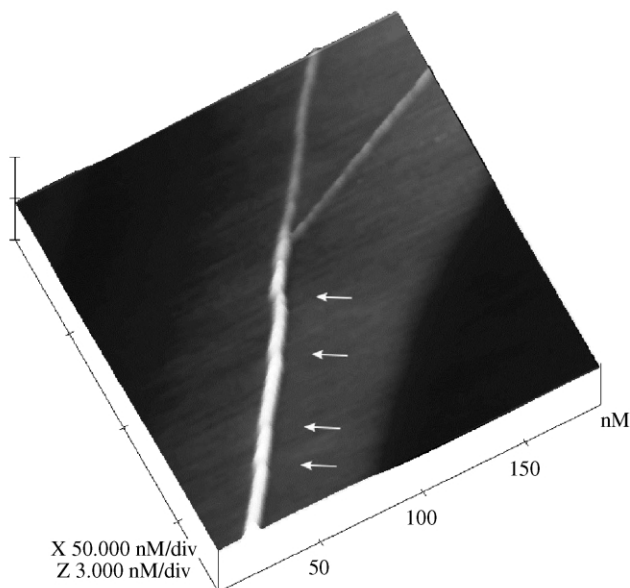


Fig. 3. Topographic STM image of an arc grown asymmetric Y junction [24] shown in 3D. Some of the growth instabilities causing minor changes in the growth direction before the Y branching occurred are marked by white arrows.

ingly small diameters in the range 0.5–0.7 nm [28], which clearly must be single wall ones. From spatially resolved spectroscopic data, by plotting the  $dI/dV$  quantity as a function of bias voltage and position along the tube, the authors conclude the existence of metallic-semiconductor junctions in the region where the three nanotube building up the Y are joined together [28].

### 3.1.2. Catalytic growth

In the past 3 years most of the works reporting the growth of the Y junctions were using some variation of the catalytic vapor deposition (CVD) method. The quality of the grown junctions shows wide scattering.

Using microwave plasma enhanced catalytic vapor deposition and Pd catalyst, partially Pd filled, multiwall carbon nanotubes were grown on a porous Si support [29], in methane/hydrogen atmosphere. Some of the tubes show Y junctions. The authors propose a root growth mechanism for the formation of Y junctions in which the molten catalyst particles on the top of two neighboring carbon nanotubes are fused together and the growth continues like a single tube.

The formation of Y branched carbon nanotubes and of multiple branchings in a proportion of 70% is reported by Satishkumar et al. [8]. Nickelocene is used as both catalyst source and carbon feedstock in combination with hydrogen bubbled through thiophene in argon carrying gas, the growth apparatus consists of a two furnace system, the nickelocene is sublimed at 623 K in the first furnace, while the growth of the Y junctions takes place at the outlet of the second furnace kept at

1273 K. The Y junctions are constituted of multiwall, relatively straight tubes, in general of similar diameters in the range of 40 nm, with a well developed and clearly visible central hollow (Fig. 4a). As revealed by HRTEM the Y junctions have a ‘fish-bone’ structure, i.e. the graphitic layers are not oriented parallel with the axis of the nanotubes constituting the junction, but rather under a certain angle. It is remarkable that even given this structure, the STS spectroscopy measurements performed on one branch of a junction show a symmetric  $dI/dV$ , while at the joining point an asymmetric characteristic is found [8]. The authors attribute the formation of the Y junctions to the catalytic effect of the thiophene present in the gas mixture. In a subsequent work [30] from the Rao group, the cobaltocene, ferrocene, Ni- and Fe-phtalocyanines and Ni(Fe)/SiO<sub>2</sub> were found to yield Y junctions under identical conditions as above. Multiple branching was observed, too, (Fig. 4c), but the junctions continue to show fish-bone structure.

Y junctions with a shorter and two longer straight arms that can reach up to 10  $\mu\text{m}$  in length, and often exhibiting multiple branching were grown using MgO supported Co catalyst in a H<sub>2</sub>/CH<sub>4</sub> gas mixture at a temperature of 1000 °C [31]. The branches of the Y junction usually have similar diameters and they are oriented at angles close to 120°. The three tubes joined in the Y have hollow cores and in general an amorphous, triangularly-shaped particle, consisting of Ca, Si, Mg and O is found at the joining of the hollow cores (Fig. 4b). It is suspected that Ca and Si are introduced as impurities in the starting materials. It is frequently

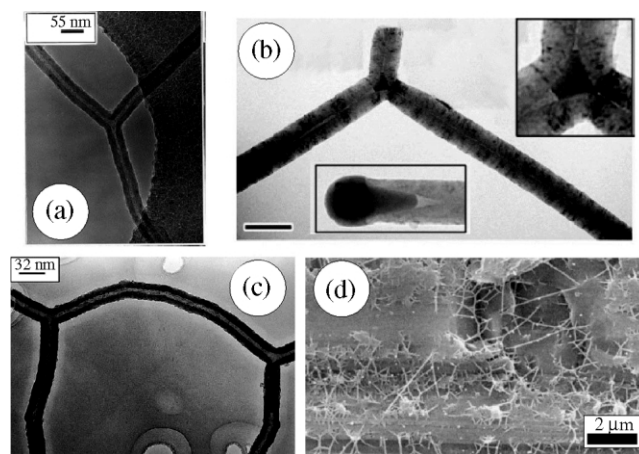


Fig. 4. Some remarkable experimental achievements by CVD growth of Y junctions. (a) Multiwall, symmetric Y junctions with well developed central hollow [8]; (b) Y junction with the triangular amorphous particle at the joining of the branches (the particle is shown in detail in the right-upper inset), central inset shows the pearl-shaped particle at the end of the branch [31] (scale bar 100 nm); (c) double Y junction grown using the pyrolysis of thiophene over Ni/SiO<sub>2</sub> catalyst [30]; (d) SEM image of an area showing several multi-junction tubes grown on scratched Si using Fe powder as catalyst [33].

observed that one of the two long arms of the Y junction is capped with a pearl-shaped particle, which has the same chemical composition as that of the triangle-shaped particle, (Fig. 4b). Sometimes a trace amount of Co was found on the surface of the pearl-shaped particle. HRTEM investigation revealed that far from the junction the branches show a tubular arrangement of the graphene layers, with satisfactory graphitization. The authors conclude that the growth is promoted by the pearl-shaped particles observed at the end of the arms, which originate by splitting due to thermal fluctuations from the triangular particle at the junction.

Y junction carbon nanotubes have been grown by hot-filament chemical vapor deposition using a tungsten filament heated at 2200 °C for which a gas mixture of acetone and hydrogen was fed and in situ evaporated copper from a copper plate placed under the hot filament was supplied [32]. TEM investigation revealed that under optimized growth conditions the fraction of Y junctions is as high as 30%, usually a thicker stem branches in two thinner arms separated at angles between 50 and 80°. HRTEM reveals fish-bone structure in the junction. If no copper is supplied during growth, no nanotubes are observed.

Multijunction carbon nanotube networks, Fig. 4d, containing Y and H junctions with regular, straight arms, were grown on 600-grit sand paper scratched Si substrates using iron powder placed in a quartz boat upstream of the substrate as catalyst source, and the pyrolysis of methane at 1100 °C as carbon source [33]. The branches have uniform diameters in the range of 30–50 nm.

### 3.1.3. Growth using template

The first experiment achieving the controlled growth of carbon nanotube Y junctions was based on the use of alumina templates with branching nanochannels [1]. Cobalt catalyst was electrochemically deposited at the bottom of the nanochannels then the pyrolysis of acetylene was carried out at 650 °C. The grown Y junctions have stems of 3- $\mu\text{m}$  length with a diameter of 90–100 nm, followed by branches of 2  $\mu\text{m}$  with diameters of 35–60 nm making a very sharp angle. HRTEM investigation of the tube walls reveals fish-bone structure. Electric transport measurements of individual Y junctions placed over Au electrodes, with the branches connected to the same electrode showed rectifying behavior [20]. Similar results were obtained for arrays of Y junctions constituted of several hundreds of individual nano-objects, while no rectification was found for arrays of straight carbon nanotubes measured under identical conditions.

A very similar growth procedure was carried out at somewhat lower temperature, 550 °C and adding hydrogen to the gas mixture. Multibranching junctions were

grown in nanochannels which were purposely etched in way that gives multibranching structure [34].

### 3.1.4. Growth by fullerene decomposition

During the electric arc, or laser ablation growth of carbon nanotubes, small carbon clusters are formed in the hot plasma, which under favorable conditions will aggregate into straight or kinked carbon nanotubes. On the other hand, such carbon clusters may be formed at much lower temperatures than that typical for electric arc or laser ablation, for example by fullerene decomposition in the presence of transition metals at temperatures in the range of 450 °C [35]. The pure carbon beam, if directed onto a highly oriented pyrolytic graphite (HOPG) surface in certain cases leads to the growth of complex nanoarchitectures, like carbon nanotube Y junctions, regularly coiled carbon nanotubes and combinations of these structures [6,36,37], (Fig. 5a). A completely symmetric Y junction, with arms oriented at 120° is shown in Fig. 5b. The carbon nanotube Y junctions grown by this technique are usually single or few wall junctions for which the possibility of the fish-bone structure can be ruled out due to the small thickness of the tube walls. Mass spectrometry has shown that in the low temperature pure carbon beam, there are present not only small  $C_{2n}$  clusters [35], but also clusters with masses in the range of  $C_{117}$  and  $C_{174}$  [38]. It is speculated that these large clusters, after soft-landing on the HOPG surface may take configurations, which promote the growth of Y junctions and other tubular forms of carbon containing n-H rings, like coils and double coils [39].

### 3.1.5. Welded junctions

Experiments carried out in situ at high temperatures (800 °C) in a high acceleration voltage TEM (1.25 MV, JEOL ARM-1250, beam intensity of  $\approx 10 \text{ A/cm}^2$ ), supported by molecular dynamic calculations, show that due to interlinking of dangling bonds created by electron irradiation, it is possible to weld together crossing singlewall carbon nanotubes and to produce Y, X, T and H junctions [40] (Fig. 6). By careful electron irradiation, it is possible to remove one arm of an X junction to transform it into a Y junction. Although the experimentally obtained junctions appear to a certain extent defective and their atomic arrangement might deviate from the idealized molecular models, the observed junctions show the expected topologies. Tight binding molecular dynamics calculations were carried out, the simulation of two crossing tubes under irradiation at 1000 °C revealed the nanotube merging process, resulting in an almost perfect molecular junction.

## 3.2. Electronic transport measurements

### 3.2.1. Transport along the junction

Although many various methods have been used to grow Y junctions, much less experimental data are

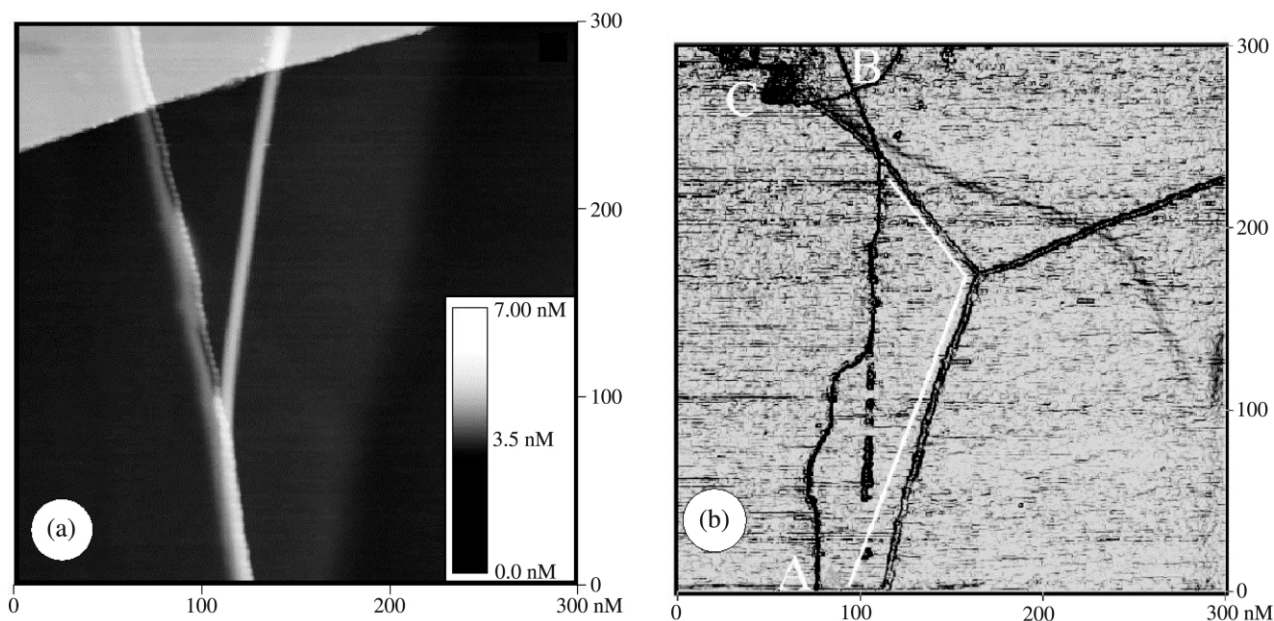


Fig. 5. Top view, topographic STM images of carbon nanotube Y junctions grown from carbon clusters produced by fullerene decomposition in the presence of transition metals. (a) Y junction and regular nanotube coil laying over it, [37]; (b) top view STM image with artificial illumination of a completely symmetric Y junction, with arms oriented at  $120^\circ$ , the irregular line AB is a cleavage step, while in C a surface defect is seen, the white lines indicate the  $120^\circ$  angle [36].

available on their conduction properties. This seems to be related to the difficulty of precisely contacting a given nano-object. A very ingenious method to measure conduction through the Y junctions grown in the nanochannels of an alumina template give solid evidence on the rectifying behavior of arrays of such junctions, averaging over large numbers 100–10 000 of individual junctions connected in parallel [20]. Arrays of straight tubes under identical experimental conditions exhibited linear  $I$ – $V$  characteristic. The Y junctions were measured with their thinner branches connected to the same grounded Al electrode, while the stems were connected to an Au electrode. For positive bias applied to the Au electrode no current, or only weak leakage current is measured, while for negative stem polarity currents of 300 mA were measured at  $-2$  V bias for an array of 100 junctions. In an experiment carried out with a single junction chemically removed from the growth template and placed over preformed Au electrodes, after a period of contact resistance reduction due to gold electromigration, similar characteristic was measured between two Au contacts as for the arrays between Al/Au contacts. The experimental findings are interpreted in the framework of the Anderson model [41] for semiconductor heterojunctions. On the basis of STS data for straight multiwall carbon nanotubes [42] showing that the gap of semiconductor tubes is proportional to the inverse of tube diameter, it is inferred that the stem has smaller gap than the two arms. This will cause depletion on the branch side of the junction. The current through the

junction can be written as [20]

$$I \sim \exp(eV/\eta k_B T), \quad (1)$$

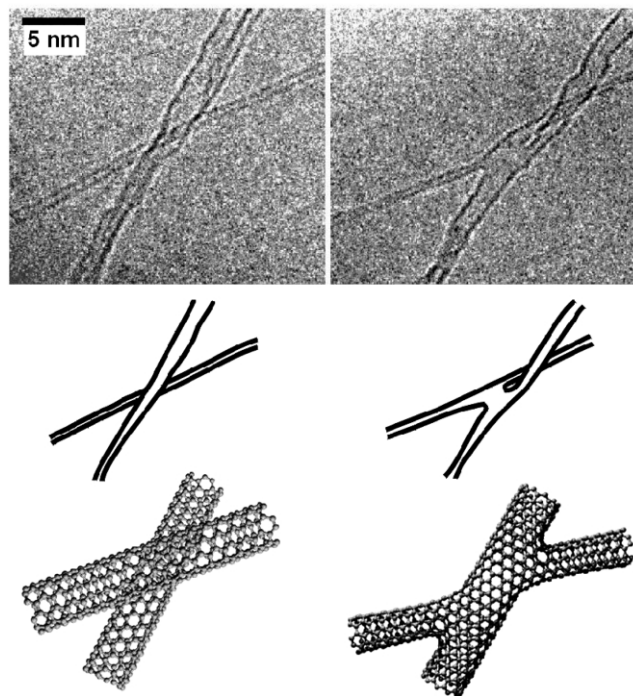


Fig. 6. Carbon nanotube junctions welded in situ under the electron beam in the TEM [40].

where  $e$  is the electronic charge,  $V$  is the bias across the junction,  $\eta = 1 + \varepsilon_2 N_2 / \varepsilon_1 N_1$  a parameter depending on the material properties on the two sides of the junction,  $k_B$  the Boltzmann constant,  $T$  the absolute temperature; with  $\varepsilon_1$  and  $\varepsilon_2$  the corresponding dielectric constants and  $N_1$  and  $N_2$  the equilibrium concentrations of the holes in the stem (branch) far from the junction. It was found that the experimental  $I$ – $V$  data are in good agreement with Eq. (1).

### 3.2.2. Transport across the branches and the junction

Tunneling conductance measurements were carried out on a CVD grown Y junction by positioning a tip over the arm and over the joining point of the branches [8]. While over the arm a symmetric  $I$ – $V$  curve was recorded in the branching region the  $I$ – $V$  curve shows asymmetry, smaller currents being measured for negative polarity than for positive polarity.

STS measurements carried out under UHV on an asymmetric single wall Y junction produced in electric arc revealed changes in the electronic properties in the vicinity of the junction [28]. Spectroscopic data were recorded as a function of bias voltage and position along the tubes, the data represented as gray scale tunneling conductance maps reveal that the region connecting the three branches exhibits metallic-type behavior and its  $dI/dV$  curve shows peaks in the range of  $\pm 1.0$  to  $\pm 1.25$  V with respect to the Fermi level. The measurements along the branches clearly show the gradual change towards the spectrum characteristic for the junction region as the measurement points are approaching to this region.

## 4. Discussion

One of the general conclusions that may be formulated after the review of the experimental data is that taking into account the very different methods which yielded in some occasions very similar nanotube Y junctions, the research community should accept these nano-object as ‘regular members’ of the carbon nanostructures family. A certain grouping of the methods may be attempted, although, for some growth methods the available data are very scarce.

The most well represented group is constituted by the Y junctions grown by CVD. Most frequently, these junctions exhibit a fishbone structure which may suggest a growth mechanism based on the fragmentation of the catalyst particle as proposed in Ref. [31]. On the other hand, the experiments by Rao and co-workers [30] convincingly demonstrate that various catalyst are suitable for the formation of Y junctions and that the presence of sulfur may be beneficial for the formation of these junctions by the catalytic route. However, the mechanism by which sulfur promotes the branching is not clear at the moment. The very dramatic changes

sulfur may induce in the growth of carbon nanostructures when transition metal catalysts are used has been pointed out by several researchers [43,44] many years ago. More recently, the role of sulfur seems to be very important in the growth of doublewall carbon nanotubes (DWCNTs) [45,46], in the absence of sulfur only SWCNTs are produced, while minute amounts of S yield DWCNTs. Sulfur can easily combine with carbon in the gas phase to form S-rich clusters and sulfur may enhance the catalytic activity of transition metals, and it may enhance the metal filling of carbon nanotubes too [44].

On the other hand, there are CVD methods, which seem to produce Y junctions, that do not have fishbone structure [31]. In these methods, like in Refs. [31,33], sulfur is not introduced intentionally, but it may not be excluded that sulfur traces may have been present along with Ca and Si, also introduced unintentionally [31]. The junctions, reported by Ren and co-workers do not have a fishbone structure, therefore they can be treated like the multiwall carbon nanotubes, at least, far from the junction. In the case of fish-bone structure it is not straightforward to apply the models used for describing the physical properties of carbon nanotubes, in which the graphene sheets are oriented along the tube axis. The fish-bone structure is more frequently encountered in graphitic fibers. As in Ref. [33] no TEM images are given, one cannot decide, if it may be inferred that the absence of sulfur promotes the growth of well graphitized Y junctions, but certainly this is one point worth to be investigated further.

There are too few results concerning the arc growth of Y junctions for attempting to extract general rules from the results. Both multiwall and singlewall junctions have been grown. The single or few wall junctions are attractive because their wall thickness does not allow for fish-bony structure. It is worth investigating in more detail, if during the arc discharge growth of single wall nanotubes, in the cathodic deposit, or in the mantle surrounding it (which contains a large variety of different carbon nanostructures [43]) Y junctions may be regularly produced. Usually, when the growth of SWCNTs is aimed the cathodic deposit is disregarded.

There is no doubt that, at the present moment, the use of nanochannel templates is the most suitable way to produce large amounts of similar Y junctions. However, it may be difficult to apply to these nanostructures the formalism developed to describe the physical phenomena occurring in well-graphitized carbon nanotubes. It is encouraging that the  $I$ – $V$  characteristic of these nanostructures shows rectifying behavior as mentioned above.

The two ‘exotic’ methods, the e-beam welding of straight carbon nanotubes and the growth by fullerene decomposition, may prove useful for fundamental studies, but it is doubtful that they will gain importance as

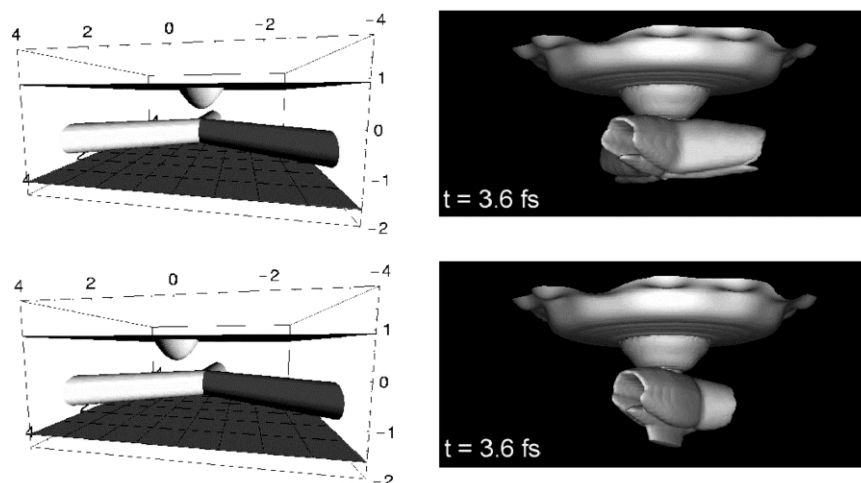


Fig. 7. Wave packet dynamical simulation of geometric effects during the tunneling through a carbon nanotube Y junction placed between the STM tip and a conductive support [47]. Right column: arrangement of the STM tip, Y junction and support. Left column: snapshots of the tunneling process at 3.6 fs. Note that even when the STM tip is placed off-junction a significant amount of charge flows in the junctions region, thus ‘sampling’ the localized states existing there due to the n-H rings.

practical ways of producing large amounts of Y junctions.

As already discussed in some detail concerning ideal singlewall junctions above, a widely accepted theoretic description is lacking at the moment. The experimental data concerning the transconduction of the Y junctions regard mainly the junctions grown in alumina templates that have shape and structure somewhat far from that of the model structures used in the calculation. When performing STS measurements on the Y junctions, some care has to be taken, due to the geometric effects inherently introduced by the presence of the junction [47] (Fig. 7) and due to effect of the n-H rings, which must be present in the junction region, on the STS curves [48]. One may observe in Fig. 7 that even when the STM tip is not placed right over the center of the junction region due to the spreading of the wave packet tunneling into one of the branches of the Y junction, the STS measurement will ‘sample’ the junction region, too. This may be the mechanism by which the localized states caused by the n-H rings affect the STS measurements in Ref. [28].

## 5. Conclusions

In accordance with early theoretical predictions, in the last years, stable carbon nanotube Y junctions have been produced by various methods. The status of the field is to some extent similar to that of the field of straight carbon nanotubes a decade ago, in the sense that the first pieces of a challenging puzzle have been identified, but a lot of efforts are needed to put together the whole picture. A better understanding and increased reproducibility for the growth methods has to be achieved and very clearly, once the Y junctions are

available on a regular basis many more efforts are needed to understand their electronic properties. It seems to be worthwhile to undertake to these challenging tasks due to very exciting application possibilities of Y junctions in nanoelectronics and in composites.

## Acknowledgments

This work was supported by the EC, contract NANOCOMP, HPRT-CT-2000-00037 and, EU5 Center of Excellence ICAI-CT-2000-70029 and by Hungarian OTKA Grant T 043685 and by the IUAP research project P5/01 on ‘Quantum-size effects in nanostructured materials’ of the Belgian Office for Scientific, Technical, and Cultural Affairs, LPB and GIM gratefully acknowledge financial support from FNRS in Belgium.

## References

- [1] J. Li, Ch. Papadopoulos, J. Xu, *Nature* 402 (1999) 253.
- [2] P. Nagy, R. Ehlich, L.P. Biró, J. Gyulai, *Appl. Phys. A* 70 (2000) 481.
- [3] S. Amelinckx, X.B. Zhang, D. Bernaerts, X.F. Zhang, V. Ivanov, J.B. Nagy, *Science* 265 (1994) 635.
- [4] L.P. Biró, G.I. Márk, A.A. Koós, J.B. Nagy, Ph. Lambin, *Phys. Rev. B* 66 (2002) 165405.
- [5] D.Y. Ding, J.N. Wang, Z.L. Cao, J.H. Dai, F. Yu, *Chem. Phys. Lett.* 371 (2003) 333.
- [6] P. Nagy, R. Ehlich, L.P. Biró, J. Gyulai, *Appl. Phys. A* 70 (2000) 481.
- [7] L.P. Biró, R. Ehlich, Z. Osváth, et al., *Mater. Sci. Eng. C* 19 (2002) 3.
- [8] B.C. Satishkumar, P. John Thomas, A. Govindaraj, C.N.R. Rao, *Appl. Phys. Lett.* 77 (2000) 2530.
- [9] F. Fehill, J.G. Vos, S. Benrezzak, et al., *J. Am. Chem. Soc.* 124 (2002) 13694.
- [10] U. Dettla-Weglikowska, J.-M. Benoit, P.-W. Chiu, R. Graupner, S. Lebedkin, S. Roth, *Curr. Appl. Phys.* 2 (2002) 497.

- [11] G.E. Scuseria, *Chem. Phys. Lett.* 195 (1992) 534.
- [12] L.A. Chernozatonskii, *Phys. Lett. A* 172 (1992) 173.
- [13] S. Iijima, *Nature* 354 (1991) 56.
- [14] M. Menon, D. Srivastava, *Phys. Rev. Lett.* 79 (1997) 4453.
- [15] G. Treboux, P. Lapstun, K. Silverbrook, *Chem. Phys. Lett.* 306 (1999) 402.
- [16] A.N. Andriotis, M. Menon, D. Srivastava, L. Chernozatonskii, *Appl. Phys. Lett.* 79 (2001) 266.
- [17] A.N. Andriotis, M. Menon, D. Srivastava, L. Chernozatonskii, *Phys. Rev. Lett.* 87 (2001) 66802.
- [18] A.N. Andriotis, M. Menon, D. Srivastava, L. Chernozatonskii, *Phys. Rev. B* 65 (2002) 165416.
- [19] V. Meunier, M. Buongiorno Nardelli, J. Bernholc, Th. Zacharia, J.-Ch. Charlier, *Appl. Phys. Lett.* 81 (2002) 5234.
- [20] C. Papadopoulos, A. Rikitin, J. Li, A.S. Vedenev, J.M. Xu, *Phys. Rev. Lett.* 85 (2000) 3476.
- [21] R. Landauer, *Z. Phys. B: Condens. Matter* 68 (1987) 217.
- [22] P.G. Collins, K. Bradley, M. Ishigami, A. Zettl, *Science* 287 (2000) 1801.
- [23] D. Zhou, S. Serapin, *Chem. Phys. Lett.* 238 (1995) 286.
- [24] Z. Osváth, A.A. Koós, Z.E. Horváth, et al., *Chem. Phys. Lett.* 365 (2002) 338.
- [25] L.P. Biró, S. Lazarescu, Ph. Lambin, et al., *Phys. Rev. B* 56 (1997) 12490.
- [26] G.I. Márk, L.P. Biró, J. Gyulai, *Phys. Rev. B* 58 (1998) 12645.
- [27] L.C. Venema, V. Meunier, Ph. Lambin, C. Dekker, *Phys. Rev. B* 61 (2000) 2991.
- [28] Z. Klusek, S. Datta, P. Byszewski, P. Kowalczyk, W. Kozłowski, *Surf. Sci.* 507–510 (2002) 577.
- [29] S.H. Tsai, C.T. Shiu, W.J. Jong, H.C. Shih, *Carbon* 38 (2000) 1879.
- [30] F.L. Deepak, A. Govindaraj, C.N.R. Rao, *Chem. Phys. Lett.* 354 (2001) 5.
- [31] W.Z. Li, J.G. Wen, Z.F. Ren, *Appl. Phys. Lett.* 79 (2001) 1879.
- [32] B. Gan, J. Ahn, Q. Zhang, et al., *Chem. Phys. Lett.* 333 (2001) 23.
- [33] J.-M. Ting, C.-C. Chang, *Appl. Phys. Lett.* 80 (2002) 324.
- [34] Y.C. Sui, J.A. Gonzalez-Leon, A. Bermudez, J.M. Saniger, *Carbon* 39 (2001) 1709.
- [35] L.P. Biró, R. Ehlich, R. Tellgmann, et al., *Chem. Phys. Lett.* 306 (1999) 155.
- [36] L.P. Biró, R. Ehlich, Z. Osváth, et al., *Diamond Relat. Mater.* 11 (2002) 1081.
- [37] A.A. Koós, R. Ehlich, Z.E. Horváth, et al., *Mater. Sci. Eng. C* 23 (2003) 275.
- [38] R. Ehlich, L.P. Biró, C. Stanciu, Z.E. Horváth, J. Gyulai, in: H. Kuzmany, J. Fink, R. Mehring, S. Roth (Eds.), *XVth International Winterschool on Electronic Properties of Novel Materials an Euroconference: Molecular Nanostructures*, vol. 591, Ser. American Institute of Physics Proceedings, American Institute of Physics, 2001, p. 175.
- [39] L.P. Biró, G.I. Márk, A.A. Koós, J.B. Nagy, Ph. Lambin, *Phys. Rev. B* 66 (2002) 165405.
- [40] M. Terrones, F. Banhart, N. Grobert, J.-C. Charlier, H. Terrones, P.M. Ajayan, *Phys. Rev. Lett.* 89 (2002) 075505.
- [41] R.L. Anderson, *Solid-State Electron.* 5 (1962) 341.
- [42] C.H. Olk, J.P. Heremans, *J. Mater. Res.* 9 (1994) 259.
- [43] C.-H. Kiang, M.S. Dresselhaus, R. Beyers, D.S. Bethune, *Chem. Phys. Lett.* 259 (1996) 41.
- [44] N. Demoncy, O. Stéphan, N. Brun, C. Colliex, A. Loiseau, H. Pascard, *Synthetic Metals* 103 (1999) 2380.
- [45] L. Ci, Z. Rao, Z. Zhou, et al., *Chem. Phys. Lett.* 359 (2002) 63.
- [46] Z. Zhou, L. Ci, X. Chen, et al., *Carbon* 41 (2003) 337.
- [47] G.I. Márk, L.P. Biró, J. Gyulai, Ph. Lambin, in: H. Kuzmany, J. Fink, M. Mehring, S. Roth (Eds.), *XVth International Winterschool on Electronic Properties of Novel Materials an Euroconference: Molecular Nanostructures*, vol. 633, American Institute of Physics, Melville, New York, 2002, p. 381.
- [48] J.-C. Charlier, *Accounts Chem. Res.* 35 (2002) 1063.